Consistent analysis of all-inclusive deuteron-induced reactions at low energies

M. Avrigeanu and V. Avrigeanu
Horia Hulubei National Institute for Physics and Nuclear Engineering, P.O. Box MG-6, 077125 Bucharest-Magurele, Romania

Abstract
An extended analysis of the reaction mechanisms involved within deuteron interaction with nuclei, namely the breakup, stripping, pick-up, pre-equilibrium emission, as well as the evaporation from fully equilibrated compound nucleus, is presented. The overall agreement between the measured data and model calculations validates the description of nuclear mechanisms taken into account for the deuteron-nucleus interaction.

1 Introduction

The description of deuteron-nucleus interaction represents an important test for both the appropriateness of reaction mechanism models and evaluation of nuclear data requested especially by the ITER [1], IFMIF [2] and SPIRAL2-NFS [3] research programmes. The weak binding energy of the deuteron, B=2.224 MeV, is responsible for the high complexity of the interaction process that supplementary involves a variety of reactions initiated by the neutron and proton following the deuteron breakup (BU). The difficulties to interpret the deuteron-induced reaction data in terms of the usual reaction mechanism models have recently been re-investigated [4–10] looking for a consistent way to include the breakup contribution within the activation cross section calculations too.

On the other hand, the (d,p) and (d,n) stripping as well as the (d,t) pick-up direct reaction (DR) contributions have also been usually neglected or very poorly taken into account, in spite of being important at low incident energies (e.g., Refs. [4–10]). Finally, the reaction mechanisms such as the pre-equilibrium emission (PE) and evaporation from fully equilibrated compound nucleus (CN) become important when the incident energy is increased above the Coulomb barrier. Actually even the PE and CN analysis has to take into account the decrease of the deuteron total reaction cross section due to above-mentioned BU, stripping and pick-up processes. The present work concerns a deeper understanding, all together and consistently, of the deuteron breakup, stripping and pick-up reactions, and the better-known statistical emission.

2 Deuteron breakup effects on activation cross sections

The physical picture of the deuteron-breakup in the Coulomb and nuclear fields of the target nucleus considers two distinct chains, namely the elastic-breakup (EB) in which the target nucleus remains in its ground state and none of the deuteron constituents interacts with it, and the inelastic-breakup or breakup fusion (BF), where one of these deuteron constituents interacts with the target nucleus while the remaining one is detected.

An empirical parametrization of the total proton-emission breakup fraction $f_{BU}^{(p)} = \sigma_{BU}^{p}/\sigma_R$, of the deuteron total reaction cross section σ_R, and the elastic breakup fraction $f_{EB} = \sigma_{EB}/\sigma_R$ were obtained [4] through analysis of the experimental systematics [11,12] of the proton-emission spectra and angular distributions of deuteron-induced reactions on target nuclei from Al to Pb, at incident energies from 15 to 80 MeV. Their dependence on the deuteron incident energy E, and charge Z and atomic number A of the target nucleus is [4]:

$$f_{BU}^{(p)} = 0.087 - 0.0066Z + 0.00163ZA^{1/3} + 0.0017A^{1/3}E - 0.000002ZE^2, \quad (1)$$

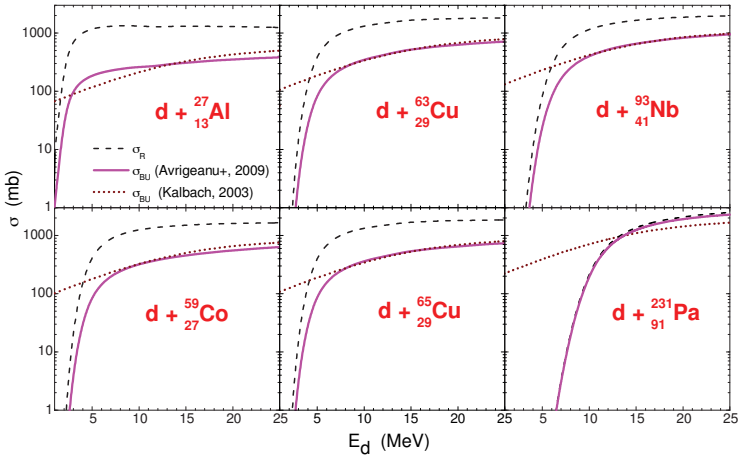

Fig. 1: The energy dependence of the deuteron total reaction cross section (dashed curves) and total breakup cross sections given by parametrizations of Avrigeanu *et al*. [4] (solid) and Kalbach [13] (dotted) for deuteron interactions with the ^{27}Al, ^{63,65}Cu, ^{59}Co, ^{93}Nb, and ^{231}Pa target nuclei.

$$f_{EB} = 0.031 - 0.0028Z + 0.00051ZA^{1/3} + 0.0005A^{1/3}E - 0.000001ZE^2. \quad (2)$$

Consequently, it results the inelastic breakup fraction

$$f^p_{BF} = f^p_{BU} - f_{EB} \quad , \quad (3)$$

and the corresponding nucleon inelastic–breakup cross sections, under the assumption that the inelastic–breakup cross section for neutron emission σ^n_{BF} is the same as that for the proton emission σ^p_{BF},

$$\sigma^{n/p}_{BF} = f^{(n/p)}_{BF}\sigma_R \quad . \quad (4)$$

A comparison with the total proton- and neutron-emission breakup cross-section parametrization of Kalbach [13],

$$\sigma^b_{BU} = K_{d,b}\frac{(A^{1/3}+0.8)^2}{1+exp\frac{(13-E)}{6}}, \;\; K_{d,p} = 21, \;\; K_{d,n} = 18 \;\; , \quad (5)$$

shows that the former parametrization [4], that considers equal breakup fractions for proton and neutron emission, supplementary provides all breakup components by means of the total, f^b_{BU}, elastic, f_{EB}, and inelastic f^b_{BF} fractions.

The comparison of the total breakup cross sections predicted by Avrigeanu *et al*. [4] and Kalbach [13] with the deuteron reaction cross sections for target nuclei from Al to Pa is shown in Fig. 1. Regardless of the differences between them, both parameterizations predict the increasing role of deuteron breakup with increasing the target nucleus mass/charge, pointing out the dominance of the breakup mechanism at the deuteron incident energies below and around the Coulomb barrier of, e.g., ^{231}Pa.

2.1 Phenomenological EB versus CDCC formalism

Concerning the energy dependence of the EB and BF components, the interest on deuteron activation cross sections for incident energies up to 60 MeV motivated an additional check [14] of the EB parameterization extension beyond the energies formerly considered for the derivation of its actual form. Actually, our parameterization [4] for the elastic-breakup was obtained through analysis of the empirical

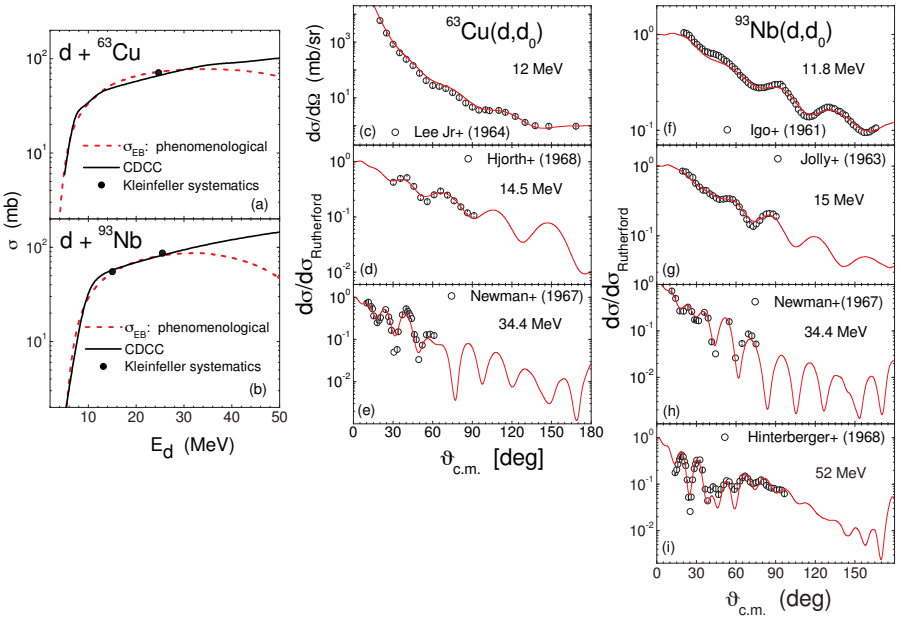

Fig. 2: (a,b) Energy dependence of empirical [4] (dashed curves) and CDCC [14] (solid) elastic breakup cross sections for deuterons on ^{63}Cu and ^{93}Nb target nuclei, and values of Kleinfeller systematics [11]. (c-i) Comparison of measured [20] and calculated (CDCC) angular distributions of deuteron elastic scattering on ^{63}Cu and ^{93}Nb.

systematics which covers an incident energy range from 15 to only 30 MeV. However, as it is shown in Fig. 2(a,b) for (a) the ^{63}Cu and (b) ^{93}Nb target nuclei, the elastic-breakup cross sections given by the empirical parameterization [4] decrease with the incident energy beyond the energy range within which it was established, while the total-breakup cross section has an opposite trend. Therefore, in the absence of available experimental deuteron elastic-breakup data at incident energies above 30 MeV, the correctness of an eventual extrapolation should be checked by comparison of the related predictions with results of a theoretical model as, e.g., the Continuum-Discretized Coupled-Channels (CDCC) method [15–18].

The elastic-breakup component is treated within the CDCC formalism as an inelastic excitation of the deuteron, coupling its unbound excited states in the solution of the scattering problem by means of the coupled channels approach. In order to deal with a finite set of coupled equations, the *binning* method [15, 16] has been used. The energy dependence of the EB cross sections provided by the excitation of the continuum spectrum (e.g the population of the virtual excited states) in the case of the deuteron interaction with ^{63}Cu and ^{93}Nb target nuclei, is compared with the prediction of empirical systematics [4] in Fig. 2(a,b). The calculations were performed with the coupled-channels code FRESCO [19]. The EB cross sections corresponding to the Kleinfeller *et el.* systematics (Table 3 of Ref. [11]) are also shown. The agreement of the CDCC elastic-breakup cross sections [14] and the latter systematics can be considered as a validation of the present advanced model approach. Moreover, the comparison shown in Fig. 2(a,b) points out that the CDCC calculations lead to EB cross sections that follow the total-breakup cross section behavior, and makes clear that the empirical parameterization extrapolation for the EB cross sections beyond the energies considered in this respect should be done with caution [14].

On the other hand, the check of the reliability of the CDCC parameters is given by the comparison between the experimental and CDCC deuteron elastic-scattering angular distributions. Therefore, the good agreement shown in Fig. 2(c-i) supports the consistent CDCC parametrization.

2.2 Inelastic-breakup enhancement of the deuteron activation cross sections

On the whole, the breakup process reduces the total reaction cross section that should be shared among different outgoing channels. On the other hand, the inelastic-breakup component, where one of deuteron constituents interacts with the target leading to a secondary composite nucleus, brings contributions to different reaction channels. Thus, the absorbed proton or neutron following the breakup emission of a neutron or proton, respectively, contributes to the enhancement of the corresponding (d, xn) or (d, xp) reaction cross sections. In order to calculate this breakup enhancement for, e.g., the (d, xn) reaction cross sections, firstly the inelastic-breakup cross sections were obtained by subtracting the EB cross sections from the phenomenological total breakup cross sections. Next, they have been multiplied by the ratios $\sigma_{(p,x)}/\sigma_R$ convoluted with the Gaussian line shape of the deuteron-breakup peak energies of the corresponding emitted constituent [21], for a given deuteron incident energy, where x stands for the γ, n, d, or α various outgoing channels [5–8].

A special point concerns the deuteron interactions with heavy nuclei, for which both breakup parameterizations [4, 13] point out the dominance of the breakup mechanism at the incident energies below and around the Coulomb barrier, as shown in Fig. 1 for deuteron interaction with ^{231}Pa target nucleus [10]. This is why recent measurements of the $^{231}\mathrm{Pa}(d,3n)^{230}\mathrm{U}$ and $^{231}\mathrm{Pa}(p,2n)^{230}\mathrm{U}$ reactions cross sections, between 11.2 and 19.9 MeV [22], and respectively 10.6 and 23.8 MeV [23], are particularly useful for the analysis of breakup effects on the former excitation function. The outgoing energy of the breakup–protons along the $^{231}\mathrm{Pa}(d,3n)^{230}\mathrm{U}$ data of Ref. [22] is covered by the $^{231}\mathrm{Pa}(p,2n)^{230}\mathrm{U}$ excitation function that can be used for the calculation of the BF enhancement of the $(d, 3n)$ reaction cross sections, as described above. Therefore, concerning the breakup mechanism dominance, it results that further calculations of deuteron activation cross sections have to take into account both the huge leakage of initial flux toward the breakup process, as well as the inelastic breakup enhancement brought by the BU nucleon interactions with the target nucleus.

These opposite effects of the breakup mechanism are shown in Fig. 3(d) for the $^{231}\mathrm{Pa}(d,3n)^{230}\mathrm{U}$ reaction. Thus, we have obtained firstly the PE and CN contributions to the $(d, 3n)$ reaction cross sections, under the assumption of no breakup process. Then the BU reduction of these results was addressed by using a reduction factor $(1 - \sigma_{BU}/\sigma_R)$ of the deuteron total reaction cross section.

Secondly, the significant BF enhancement comes from the absorbed proton, following the breakup neutron emission, through the $^{231}\mathrm{Pa}(p,2n)^{230}\mathrm{U}$ reaction. In order to calculate this breakup enhancement of the $^{231}\mathrm{Pa}(d,3n)^{230}\mathrm{U}$ reaction, the nucleon BF cross section σ^n_{BF} [10] was multiplied by the convolution of the ratio $\sigma_{(p,2n)}/\sigma_{(p,R)}$ with the Gaussian distribution of the breakup–proton energies corresponding to a given incident deuteron energy. The latest above-mentioned quantities are shown in Fig. 3(c) for three deuteron incident energies. The areas of the related convolution results correspond to the BF enhancement of the $(d, 3n)$ reaction cross sections at the given deuteron energies. The energy dependence of this BF enhancement of the $^{231}\mathrm{Pa}(d,3n)^{230}\mathrm{U}$ activation cross section is shown by dot-dashed curve in Fig. 3(d), while the corresponding total activation of ^{230}U is finally compared with the experimental data [22]. The realistic treatment of the BF enhancement by taking into account the quite large widths Γ of the breakup–proton energy distributions, shown in Fig. 3(a), has led to a rather accurate description of data. Further improvements of the breakup analysis may lead to a better account of the related energy dependence, while the present results prove the important role of breakup mechanism at the incident energies around the Coulomb barrier of a heavy target nucleus.

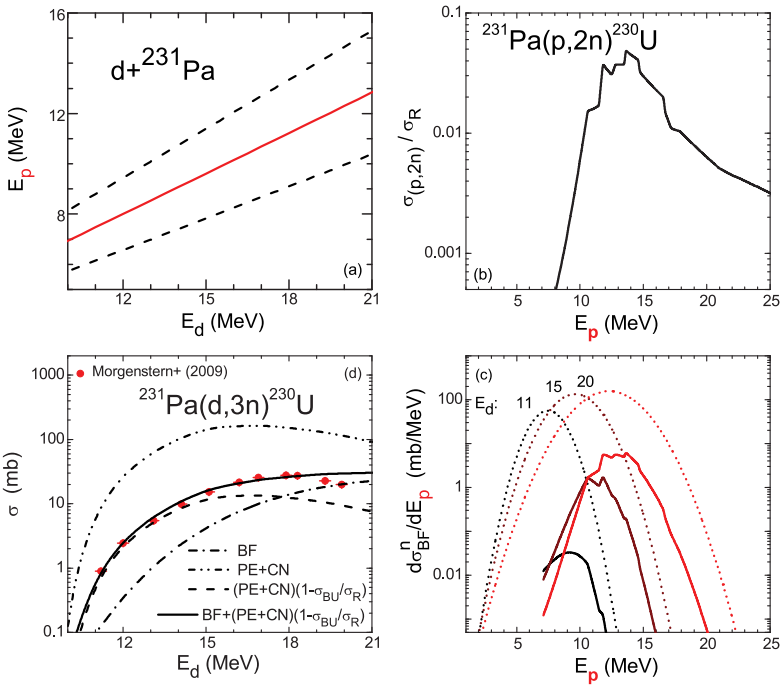

Fig. 3: (a) The centroid E_p of the Gaussian distribution of breakup-protons energies [21] versus the deuteron incident energy (solid curve) on ^{231}Pa, and the related $E_p \pm \Gamma/2$ values (dashed), (b) the cross section ratio $\sigma_{(p,2n)}/\sigma_{(p,R)}$ for the target nucleus ^{231}Pa, (c) the results (solid curves) of its convolution with the Gaussian distribution (dotted) of breakup-protons energies for deuterons on ^{231}Pa at incident energies of 10, 15 and 20 MeV noted above them, and (d) the corresponding BF enhancement (dash-dotted) of the ^{231}Pa$(d,3n)^{230}$U reaction, the PE+CN contributions to $(d,3n)$ reaction cross sections calculated without (dash-dot-dotted) and with (dashed) inclusion of the BU effect on σ_R, as well as the sum of all reaction mechanism contributions (solid).

3 One-nucleon transfer reactions

Apart from the breakup contributions to deuteron interactions, an increased attention has to be devoted to the direct reactions very poorly accounted so far in deuteron activation analysis. For low and medium mass target nuclei and deuteron energies below and around the Coulomb barrier, the interaction process proceeds largely through DR mechanism, while pre-equilibrium-emission and evaporation from fully equilibrated compound nucleus become also important with the increase of the incident energy.

The appropriate calculations of the DR contributions, like stripping and pick-up, that are important at the low energy side of the (d,p), (d,n) and (d,t) excitation functions [4–9], have been performed in the frame of the CRC formalism by using the code FRESCO [19]. The n-p interaction in deuteron [15] as well as d-n interaction in triton [24] are assumed to have a Gaussian shape, while the transferred nucleon bound states were generated in a Woods–Saxon real potential [7].

A particular note should concern the (d,t) pick-up mechanism contribution to the total (d,t) activation cross section, shown e.g. in Fig. 4(a). Usually neglected in the deuteron activation cross sections calculations, the (d,t) pick-up process is responsible for lowest-energy part of the excitation function, namely at the energies between its threshold and the (d,dn) and $(d,p2n)$ reaction thresholds, where the population of the same residual nucleus takes place [7–9].

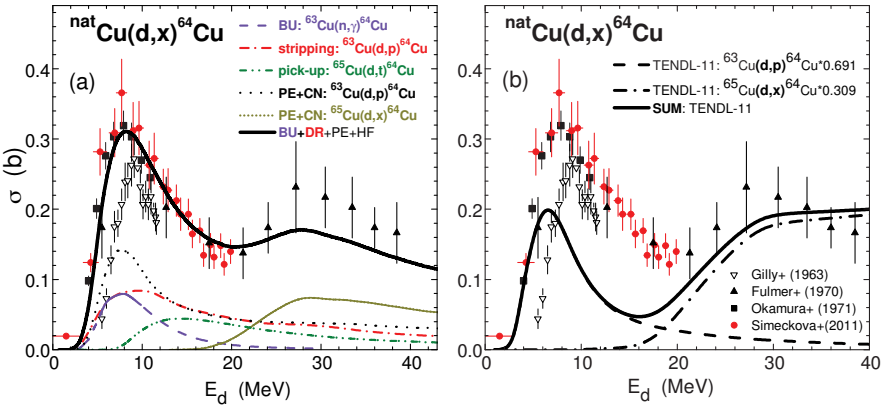

Fig. 4: Comparison of the ^{nat}Cu(d,x)^{64}Cu measured data ([7] and Refs. therein) with (a) the calculated related deuteron BF (dashed), DR stripping reaction ^{63}Cu(d,p)^{64}Cu (dash-dotted) and pick-up reaction ^{65}Cu(d,t)^{64}Cu (short dash-dot-dotted), PE+CN contributions, corrected for initial deuteron flux leakage through direct processes, to the ^{63}Cu(d,p)^{64}Cu reaction (dotted) and ^{65}Cu(d,x)^{64}Cu reaction (short-dotted), and their sum (solid curve), and (b) the corresponding TENDL-2011 predictions [27].

4 Statistical particle emission

The PE and CN reaction mechanisms become important at the incident energies above the Coulomb barrier. We have calculated the corresponding reaction cross sections by means of the codes STAPRE-H [25] and TALYS [26], taking into account also the breakup and DR results discussed above. Particularly, a consistent local parameter set was involved within the detailed analysis carried out using the code STAPRE-H [5,7].

As a sample case of complete analysis for deuteron interactions with nuclei, a comparison of the measured and calculated activation cross sections of ^{nat}Cu(d,x)^{64}Cu reaction [7] is shown in Fig. 4(a), the data being properly described by the local consistent parameter set within the PE+CN code STAPRE-H and taking into account also the breakup and DR contributions. These results substantiate the correctness of nuclear mechanism description that have been considered for the deuteron-nucleus interactions. Finally, Fig. 4(a) may be considered representative for the complexity of the deuteron interaction involving breakup, pick-up, PE and CN reaction mechanisms.

5 Conclusions

The overall agreement between the measured data and model calculations validates the description of nuclear mechanisms taken into account for the deuteron-nucleus interaction. On the other hand, the apparent discrepancies between the experimental data and corresponding TENDL-2011 [27] evaluation, shown in Fig. 4(b), stress out the effects of disregarding of the inelastic breakup enhancement, as well as of the stripping and pick-up processes.

However, while the associated theoretical frames are already settled for stripping, pick-up, PE and CN mechanisms, an increased attention should be paid to the breakup mechanism. Thus more work has to be done concerning its theoretical description including the inelastic component. The overall improvement of deuteron breakup description requires complementary experimental studies too.

Acknowledgments

This work was supported by a grant of the Romanian National Authority for Scientific Research, CNCS - UEFISCDI, project No. PN-II-ID-PCE-2011-3-0450.

References

[1] http://www.iter.org/proj.

[2] http://www.ifmif.org/b/.

[3] http://pro.ganil-spiral2.eu/spiral2/instrumentation/nfs.

[4] M. Avrigeanu *et al*., Fusion Eng. Design **84** (2009) 418.

[5] P. Bém *et al*., Phys. Rev. C **79** (2009) 044610.

[6] M. Avrigeanu and V. Avrigeanu, EPJ Web of Conf. **2** (2010) 01004; J. Phys: Conf. Ser. **205** (2010) 012014; E. Šimečková *et al*., EPJ Web of Conferences **8** (2010) 07002.

[7] E. Šimečková *et al*., Phys. Rev. C **84** (2011) 014605.

[8] M. Avrigeanu and V. Avrigeanu, J. Korean Phys. Soc. **59** (2011) 903; E. Šimečková *et al*., J. Korean Phys.Soc. **59** (2011) 1928.

[9] M. Avrigeanu and V. Avrigeanu, EPJ Web of Conf. **21** (2012) 07003.

[10] M. Avrigeanu, V. Avrigeanu, and A. J. Koning, Phys. Rev. C **85** (2012) 034603.

[11] J. Kleinfeller *et al*., Nucl. Phys. **A370** (1981) 205.

[12] J. Pampus *et al*., Nucl. Phys. **A311** (1978) 141; J. R. Wu *et al*., Phys. Rev. C **19** (1979) 370; N. Matsuoka *et al*., Nucl. Phys. **A345** (1980) 1; M. G. Mustafa *et al*., Phys. Rev. C **35** (1987) 2077.

[13] C. Kalbach Walker, TUNL Progress Report **XLII** (2002-2003) p. 82-83, Triangle University Nuclear Laboratory; www.tunl.duke.edu/publications/tunlprogress/2003/ .

[14] M. Avrigeanu and A. M. Moro, Phys. Rev. C **82** (2010) 037601.

[15] M. Kawai, M. Kamimura, and K. Takesako, Prog. Theor. Phys. Suppl. **184** (1969) 118.

[16] N. Austern *et al*., Phys. Rep. **154** (1987) 125.

[17] R. A. D. Piyadasa *et al*., Phys. Rev. C **60** (1999) 044611.

[18] A. M. Moro and F. M. Nunes, Nucl. Phys. **A767** (2006) 138; A. M. Moro *et al*., Phys. Rev. C **80** (2009) 054605; A. M. Moro *et al*., Phys. Rev. C **80** (2009) 064606.

[19] I. J. Thompson, Comput. Phys. Rep. **7** (1988) 167 (1988); v. FRES 2.3 (2007).

[20] L. L. Lee Jr. and J. P. Schiffer, Phys. Rev. **134** (1964) B765; EXFOR C1024 entry; S.A. Hjorth and E.K. Lin, Nucl. Phys. **A116** (1968) 1; EXFOR C1075 entry; E. Newman, L. C. Becker, and B. M. Freedom, Nucl. Phys. **A100** (1967) 225; EXFOR C1067 entry; R. K. Jolly *et al*., Phys. Rev. **130** (1963) 2391; EXFOR C1023 entry; F. Hinterberger *et al*., Nucl. Phys. **A111** (1968) 265; EXFOR D0225 entry; G. Igo *et al*., Phys. Rev. **124** (1961) 8332; EXFOR D0239 entry.

[21] C. Kalbach Walker, in: TUNL Progress Report, vol. XLVI (2007), p. 78; www.tunl.duke.edu/publications/tunlprogress/2007/tunlxlvi.pdf;

[22] A. Morgenstern *et al*., Phys. Rev. C **80**(2009) 054612.

[23] A. Morgenstern *et al*., Anal. Chem. **80** (2008) 8763; EXFOR D0562 entry.

[24] P. Guazzoni *et al*., Phys. Rev. C **83** (2011) 044614.

[25] M. Avrigeanu and V. Avrigeanu, IPNE Report NP-86-1995, Bucharest, 1995; News NEA Data Bank **17** (1995) 22.

[26] A. J. Koning, S. Hilaire, and M. C. Duijvestijn, in *Nuclear Data for Science & Technology, Nice, 2007* (EDP Sciences, Paris, 2008); v. TALYS-1.4, Dec. 2011, http://www.talys.eu/home/.

[27] A.J Koning and D. Rochman, *TENDL-2011: TALYS-Based Evaluated Nuclear Data Library*, Dec. 29, 2011, http://www.talys.eu/tendl-2011/.